



CHALMERS
UNIVERSITY OF TECHNOLOGY

On the Sparsity and Aperiodicity of a Base Station Antenna Array in a Downlink MU-MIMO Scenario

Downloaded from: <https://research.chalmers.se>, 2026-04-06 10:49 UTC

Citation for the original published paper (version of record):

Amani, N., Maaskant, R., Van Cappellen, W. (2019). On the Sparsity and Aperiodicity of a Base Station Antenna Array in a Downlink MU-MIMO Scenario. ISAP 2018 - 2018 International Symposium on Antennas and Propagation

N.B. When citing this work, cite the original published paper.

On the Sparsity and Aperiodicity of a Base Station Antenna Array in a Downlink MU-MIMO Scenario

N. Amani¹, R. Maaskant^{1,2}, and W. A. Van Cappellen³

¹Department of Electrical Engineering, Chalmers University of Technology, Gothenburg, Sweden

²Electromagnetics Group, Eindhoven University of Technology (TU/e), Eindhoven, The Netherlands

³Radio Group, Netherlands Institute for Radio Astronomy (ASTRON), Dwingeloo, The Netherlands

Corresponding author: anavid@chalmers.se

Abstract—An application study into irregular sparse arrays (ISAs) is proposed to function as base station antennas (BSAs) in a mm-wave multi-user multiple-input multiple-output (MU-MIMO) system. The results show that the sum rate capacity of ISAs can be increased relative to regularly-spaced BSA arrays with half a wavelength element separation, especially for a high number of users. This is due to the narrower beams formed by the larger antenna apertures of sparse arrays. Furthermore, the aperiodic distribution of antenna elements alleviates the problem of grating lobes in sparse arrays and is seen to improve the average power consumption of power amplifiers at the same time.

1. Introduction

Offering higher data rates to multiple simultaneous users requires the usage of larger bandwidths, which are available at higher frequencies. Significant research on multi user multiple-input multiple-output (MU-MIMO) technology has been carried out on developing specialized signal processing and precoding algorithms [1]. However, less attention has been paid to the array architecture and its impact on the MIMO performance metrics [2]. The relatively large propagation and material losses at mm-wave frequencies, as well as other signal degrading effects, are partly compensated for by using very large effective isotropic radiated power (EIRP) levels on the base station antenna (BSA) side [3]. This can be realized by serving user equipments (UEs) with narrow pencil beams.

Sparse antenna arrays employ larger inter-element spacings as a result of which larger aperture areas are realized that are capable of forming narrower beams. However, the penalty is the appearance of grating lobes with almost an identical power level as the main lobe. Irregular arrays can alleviate the problem of high-level grating lobes [4], [5] because the inter-element spacing between adjacent elements in irregular sparse arrays (ISAs) are different, so that grating lobes of sub-arrays occur at different angles and do not add constructively; the aperiodicity in sparse arrays converts high level grating lobes into many smaller side lobes having lower power levels.

2. Irregular Sparse Array

Our study assumes a linear BSA array of twenty antenna elements operating at 28 GHz. A sparse version of the array is realized by multiplying the inter-element spacing of a conventional regularly-spaced array (0.5λ , where λ is a wavelength) by a sparsity factor (SF). The higher the SF, the narrower

the beams. The appearance of grating lobes is a source of interference for adjacent cells in the cellular network, but this effect will be alleviated by introducing array aperiodicity as explained above.

The aperiodic array layout is synthesized through a Monte Carlo simulation involving a random distribution of UEs from which the average power spread (APS) at the BSA element ports is extracted. This is done first for a very dense regular array, after which the number of elements is down-selected through a power density tapering approach [6]. Typically, the convexity of the APS can be moderated by assigning more elements to the edges of the aperture. The result is a linear ISA that is mirror symmetric with respect to its center that is capable of minimizing the spread in average power levels at its input ports.

A. Simulation Results

The 20-element linear BSA array is assumed to have a 60° sectorial field-of-view (FoV) within which UEs are randomly distributed and where the BSA-to-UE distance D ranges from one to three Fraunhofer distances (FD), i.e., $FD \leq D \leq 3FD$. The free space path loss must therefore be taken into account ($1/D$ -distance effect). The zero forcing (ZF) precoding algorithm is adopted during each Monte Carlo simulation yielding a UE positional distribution and the corresponding excitation coefficients for the BSA antenna elements. Fig. 1 depicts the case of a ZF-beamformed BSA that is placed at $x = y = 0$ and is serving three UEs within its FoV (white stars, single Monte Carlo realization). The top figure shows the normalized radiation pattern of a conventional uniform linear array with $\lambda/2$ -element spacing. The case of a sparse uniform linear array with $SF = 2$ is shown in the middle. As expected, narrower beams of similar signal strengths are formed toward the targeted users, but grating lobes appear as well. The bottom figure shows the ISA case, where the signal levels at the targeted UEs are virtually maintained, while managing to reduce the grating lobe levels at the same time. In fact, more side lobes with lower signal levels appear, while the total radiated powers are identical in all the cases.

Next, Fig. 2 shows the BSA performance gains of the ISA relative to a conventional array with $\lambda/2$ inter-element spacing, both in terms of the power amplifier power consumption (PAPC, top figure) and the sum rate capacity (SR, bottom

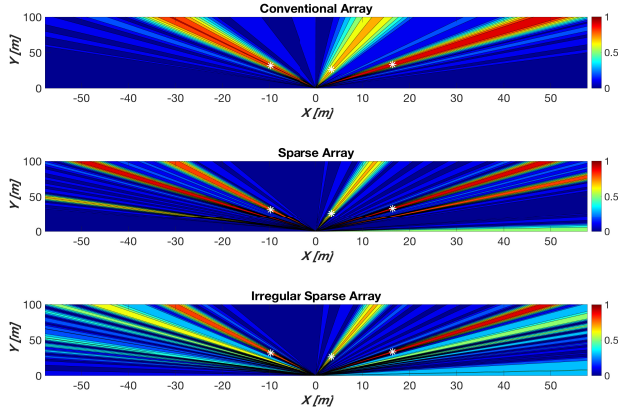


Fig. 1: Radiated power distribution in the xy -plane of a ZF-beamformed linear (top) conventional array; (middle) sparse array with SF = 2, and; (bottom) irregular sparse array.

figure), for a range of SF values and different number of UEs (K). An ISA is thus designed for each specific number of UEs and each SF value.

The PAPC calculation assumes that the maximum level of per-antenna power for each Monte Carlo simulation does not exceed the P_{1dB} value of a PA. A relation between the output power P_{output} and the Power Added Efficiency η_{PAE} of a 28-GHz SiGe BiCMOS PA is extracted from the curve in [7, Fig. 6(b)]. Since P_{input} is much smaller than P_{output} then η (drain efficiency) tends to η_{PAE} . Therefore, the PA power consumption is computed as $\text{PAPC} = P_{\text{output}}/\eta$. Hence, the PAPC ratio is

$$\text{PAPC}_{\text{ratio}} = \frac{\sum_{n=1}^{20} (\mathbb{E}\{\text{PAPC}_n^{\text{ISA}}\})}{\sum_{n=1}^{20} (\mathbb{E}\{\text{PAPC}_n^{\text{c}}\})} \quad (1)$$

where \mathbb{E} denotes the statistical expectation taken over all Monte Carlo simulations, and where $\text{PAPC}_n^{\text{ISA}}$ and PAPC_n^{c} are the power consumptions of the n th PA in the ISA and conventional array case, respectively.

The required weight vector using ZF precoding is computed for a given ISA in each run of a Monte Carlo simulation, after which the SR is calculated (SNR is assumed to be 20 dB). Accordingly, the sum rate ratio is defined as

$$\text{SR}_{\text{ratio}} = \text{SR}^{\text{ISA}}/\text{SR}^{\text{c}} \quad (2)$$

where SR^{ISA} and SR^{c} are the calculated sum rates of a MU-MIMO system when an ISA and a conventional array are employed as a BSA, respectively.

As can be seen from Fig. 2, increasing the SF improves the sum rate capacity of a MU-MIMO system owing to the narrower beams that can be formed. In addition, the irregular distribution of antenna elements in the ISA improves the PAPC, mostly for lower sparsity factors. Therefore, there will be an optimal value of SF which renders a compromise between the SR and the PAPC. For instance, when SF = 1.6, the $\text{PAPC}_{\text{ratio}}$ is seen to decrease non-monotonically from 0.94

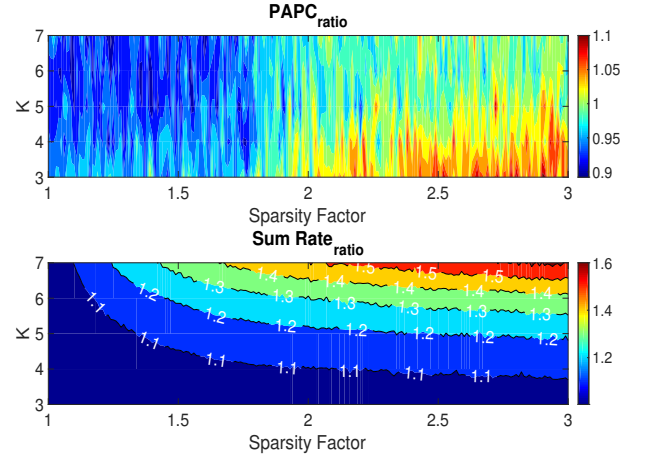


Fig. 2: Power amplifier power consumption (PAPC) and sum rate (SR) ratios.

to 0.9 when increasing the number of UEs from 3 to 7, but then the SR_{ratio} also increases from 1.03 to 1.38.

3. Conclusion

The potential application of both an irregular and sparse array (ISA) in a MU-MIMO scenario has been studied. It has been shown that the array sparsity in the BSA design can significantly improve the sum rate capacity of a MIMO system, relative to a conventional uniform linear BSA. Furthermore, the aperiodicity can mitigate the problem of grating lobes by transforming them into (more) side lobes of lower level.

Acknowledgement

This project has received funding from the European Union's Horizon 2020 research and innovation programme under the Marie Skłodowska-Curie grant agreement No 721732.

REFERENCES

- [1] H. Q. Ngo, E. G. Larsson, and T. L. Marzetta, "Energy and spectral efficiency of very large multiuser MIMO systems," *IEEE Transactions on Communications*, vol. 61, no. 4, pp. 1436–1449, April 2013.
- [2] N. Wu, F. Zhu, and Q. Liang, "Evaluating spatial resolution and channel capacity of sparse cylindrical arrays for massive MIMO," *IEEE Access*, vol. 5, pp. 23 994–24 003, 2017.
- [3] N. Amani, R. Maaskant, A. Glazunov, A. and M. Ivashina, "Network model of a 5G MIMO base station antenna in a downlink multi-user scenario," *12th European Conference on Antennas and Propagation*, 2018.
- [4] B. Smolders, "Random sparse arrays: An option for SKAI?" Citeseer, Tech. Rep., 1998.
- [5] W. Van Cappellen, S. Wijnholds, and J. Bregman, "Sparse antenna array configurations in large aperture synthesis radio telescopes," in *Radar Conference, 2006. EuRAD 2006. 3rd European*. IEEE, 2006, pp. 76–79.
- [6] P. Angeletti and G. Toso, "Array antennas with jointly optimized elements positions and dimensions Part I: Linear arrays," *IEEE Transactions on Antennas and Propagation*, vol. 62, no. 4, pp. 1619–1626, April 2014.
- [7] A. Sarkar, F. Aryanfar, and B. A. Floyd, "A 28-GHz SiGe BiCMOS PA with 32% efficiency and 23-dBm output power," *IEEE Journal of Solid-State Circuits*, vol. 52, no. 6, pp. 1680–1686, June 2017.